BNL-105584-2014-TECH

BNL/SNS Technical Note No. 007;BNL-105584-2014-IR

# Space Charge and Coherent Effects in the NSNS Storage Ring

A. G. Ruggiero

June 1996

Collider Accelerator Department

**Brookhaven National Laboratory**

**U.S. Department of Energy**

USDOE Office of Science (SC)

# DISCLAIMER

# SPACE CHARGE and COHERENT EFFECTS in the NSNS STORAGE RING

BNL/NSNS TECHNICAL NOTE
NO. 007

Alessandro G. Ruggiero

June 6, 1996

ALTERNATING GRADIENT SYNCHROTRON DEPARTMENT
BROOKHAVEN NATIONAL LABORATORY
UPTON, NEW YORK 11973

# Space Charge and Coherent Effects in the NSNS Storage Ring

Alessandro G. Ruggiero
Brookhaven National Laboratory

June 6, 1996

*Abstract*

The goal of the proposed National Spallation Neutron Source is to provide a short pulse proton beam of about 0.5 second with average beam power of 1-2 MW. To achieve such a purpose, a proton storage ring operated at 60 Hz with 1-2 x $10^{14}$ protons per pulse at 1 GeV is required. Care has been exercised to ascertain that the space charge effect at injection and coherent instabilities through the accumulation cycle are acceptable and that the final intensity can actually be achieved. Other issues addressed in this investigation are the performance upgrade potential to 2 MW and engineering requirements on system components.

## 1. Introduction

The proton storage ring is one of the major systems in the design of the National Spallation Neutral Source (NSNS) [1]. The function of the storage ring is to take the 1.0 GeV proton beam from the Linac and convert the long Linac beam of about 1 ms into a 0.5 second beam in about one thousand turns. The final beam has 1 x $10^{14}$ proton per pulse, resulting in 1 MW average beam power at 60 Hz repetition rate. Provision has been reserved for a future upgrade to 2 MW by doubling the storage beam to 2 x $10^{14}$ proton per pulse. The lattice of the storage ring is a simple FODO lattice with three-fold symmetry and the dispersion function is reduced to zero at straight sections by the missing magnet scheme. The total circumference of the ring is 208.6 m and the transition energy is 3.42, higher than the operating energy of 1 GeV to avoid the difficult instability problem that are expected above transition. The cell structure, beta-function, and dispersion function are shown in Figure 1 and the salient design parameters are shown in Table 1.

In section 2, the estimated impedance from the storage ring components will be given. In section 3, the single bunch instabilities will be investigated and the incoherent space charge effect will be studied in section 4.

## 2. Wall Impedance Budget

The frequency range and the magnitude of the wall-coupling impedance in a storage ring is determined essentially by the dimensions of the vacuum chamber and by the energy of the beam through the relativistic factor $\gamma$, the ratio of the total beam energy to the rest energy. A major feature of a low-energy storage ring is the low value of $\gamma$ and therefore of the impedance frequency range of interest. In fact the cut-off harmonic number above which the beam does not interact

effectively with the wall components is given roughly by $n_c \sim \gamma R/b$, where R is the average ring radius and b is the average vacuum chamber size. Using parameters shown in Table 1 it is seen that $n_c \sim 277$, which is a very narrow frequency range (of only 0.5 GHz) when compared to that of high-energy storage rings (SSC, LHC, RHIC, Tevatron,...). Another major feature when compared to electron beams at ultra-relativistic velocities [2], is the complete screening of the beam from interacting with the free space and therefore the inhibition of radiation. In fact the cut-off for synchrotron radiation is $n_{rad} \sim 1.5\ \gamma^3$, considerably lower than the vacuum chamber cut-off $n_c$.

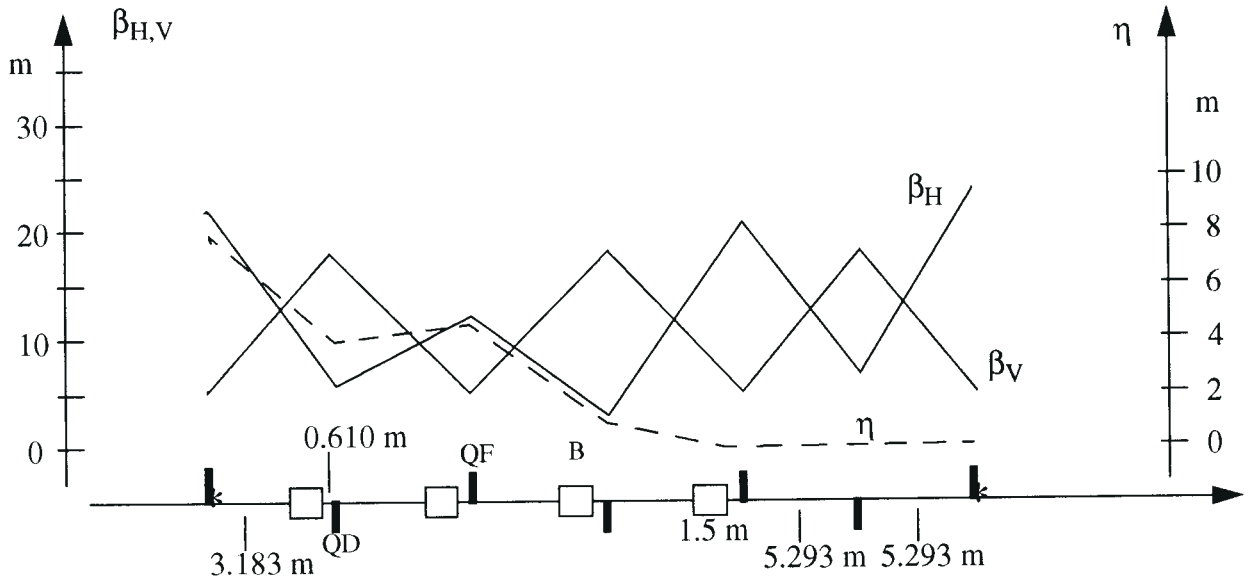


Figure 1. Half period of the NSNS accumulator ring lattice

2.1 Longitudinal coupling impedance.

A third and very important feature of a low-energy storage ring, with consequences on its stability against coherent perturbation, is the magnitude of the space-charge forces. It is customary [3] to express the beam-wall interaction by the Z/n impedance because it enters in some stability conditions. The space-charge contribution, that is the electromagnetic field stored in the region between the beam and the vacuum chamber, is then [4]

$$Z/n = i\ Z_0\ (1 + 2 \ln b/a) / 2\ \beta\ \gamma^2 \qquad (1)$$

where $Z_0 = 377$ ohm and a is the average beam radius. For the example given in Table 1, the space-charge contribution is 114 i ohm.

The expression above is estimated assuming a straight pipe. Actually, the vacuum chamber is bent, and its curvature may resonate at modes which can be excited by the beam [5]. The excitation condition is roughly given by the lowest harmonic number $n_r$ satisfying

$$\beta\ (1 + b/R) = 1 + 0.80862\ n_r^{-2/3} \qquad (2)$$

It is seen that one of the advantages of the low-energy storage ring is the absence of the vacuum

chamber resonating modes, because of the relative low value of the beam velocity $\beta$, and of the relative large ratio of pipe size b to the ring radius R.

Table 1: General Parameters of the NSNS Project

| | | |
|---|---|---|
| Average Power | 1.0 MW | 2.0 MW |
| Kinetic Energy | 1.0 GeV | |
| Circumference | 208.56 m | |
| Bending Field | 0.9874 T | |
| Number of Protons | $1.04 \times 10^{14}$ | $2.08 \times 10^{14}$ |
| Betatron Tunes, H / V | 3.82 / 3.78 | |
| Transition Energy, $\gamma_T$ | 3.422 | |
| Full Betatron Emittance | 60 $\pi$ mm mrad | 120 $\pi$ mm mrad |
| Space-Charge Tune-Shift | 0.2 | |
| RF peak Voltage (h = 1) | 13 kV | 26 kV |
| Revolution Frequency | 1.258 MHz | |
| Filling Time | 1.0 ms | |
| Synchrotron Period | 1.7 ms | 1.2 ms |
| Bunching Factor | 0.324 | |
| Bunch Area | 7 eV-s | 10 eV-s |
| Full Momentum Spread | 1.2 % | 1.7 % |
| Average Pipe Radius | 12 cm | |

The next contribution is the resistivity of the wall [6]

$$Z/n = (1 - i)\ (Z_0 \rho_w R / 2 b^2 n)^{-1/2} \qquad (3)$$

where the wall resistivity $\rho_w = 73\ \mu\Omega$ x cm for Stainless Steel. At the lowest harmonic n=1, we have Z/n = (1-i) 0.56 ohm. At the same time the skin depth is 0.38 mm. Thus a vacuum chamber thickness of 2 mm or more is adequate for screening the beam from interacting with other components outside the vacuum chamber, especially in the case when there are no fast-varying fields sources.

Next we have contributions which are caused by discontinuities of the vacuum chamber. We give below the expression of the contribution to Z/n for some of them.

Bellows:

Let M be the total number of bellows, m be the number of convolutions per bellow, h the height and w the width of each convolution, then the contribution to Z/n in the low frequency range is [7]

$$Z/n = - i Z_0 ( MmW / 2\pi R ) \ln (1 + h/b) \quad (4)$$

Each convolution resembles a cavity resonating at frequencies $f_k = (1 + 2k) c / 4 h$ ( k = 0, 1, 2,...) [8,9]. Fortunately the lowest resonating mode is well above the vacuum-chamber cut-off so that the beam is not expected to be capable to excite these modes significantly.

Strip Lines:

They can be beam position monitors or clearing electrodes. We shall assume M strip lines each made of m=2 plates of width w. The characteristic impedance is $Z_{cha}$ and the termination is matched exactly to this. The general expression of the contribution to Z/n is [10]

$$Z/n = - 4i Z_0 (Mm / n) ( w / 2\pi b )^2 \exp (-i \omega d / c) \sin ( \omega d / 2c) \quad (5)$$

where d is the length of a plate, and $\omega = n \beta c/R$. Strip lines do resonate at the harmonic number $n = c/2d$, which is at about the vacuum chamber cut-off.

Vacuum Chamber Steps:

These are the transitions from a rectangular vacuum chamber in the dipole magnets to straight cylindrical pipes in the remaining sections of the ring. Steps are assumed to be far apart, more than the pipe diameter so that are not coupled together to form a resonating cavity. The contribution to the coupling impedance is, with M the number of transitions, [11]

$$Z/n = 2 M ( 1 - i \pi ) Z_0 ( S - 1 )^2 b / 2 \pi^2 R \quad (6)$$

for $n < n_w = 2\pi R / 2b ( S - 1 )$, and for $n > n_w$

$$Z/n = Z_0 \ M ( S - 1 ) / 2\pi n \quad (7)$$

where S is the ratio of the inner dimension to the outer dimension of the step.

Vacuum Pump Ports:

These are circular openings of diameter d. The impedance is caused by the diffraction of the electromagnetic wave through them. The impedance for M ports is [12]

$$Z/n = 2 M Z_0 \alpha^2 [ n^3 + i (8/\pi) ( n^2 n_{co} + n_{co}^3 / 3 ) ] / 3 \pi^3 R^4 b^2 \quad (8)$$

where $n_{co} = 2\pi R / d$ and $\alpha = \pi d^3 / 16$

Kicker Magnets:

The contribution to Z/n from a kicker is essentially given by the amount of inductance involved. There is a resistive contribution also due to the resistivity of the coils and to the losses in the ferrite. A simple formula is

$$Z/n = -2\pi i \mu f_0 V \tau / B d w \qquad (9)$$

where $f_0$ is the revolution frequency, V the excitation voltage, $\tau$ the kicker rise time, B the field, d the length, w the width, and $\mu$ the relative permeability of the ferrite.

RF Cavities:

An rf cavity can always be approximated with an equivalent RLC parallel circuit and be described by the resonating frequency, the figure of merit Q and the shunt impedance $R_s$. In the example cited above the rf system is tuned to the revolution frequency. The impedance at the resonating frequency can be compensated with the feedback system operating at the same frequency. Care in the design choice is to be taken to make sure that the contribution of the rf system to the neighboring harmonics is not too excessive. In our example the contribution would be capacitive, and thus adds to the space-charge contribution.

Figure 2 gives a plot of the expected longitudinal coupling impedance for the example of the NSNS storage ring.

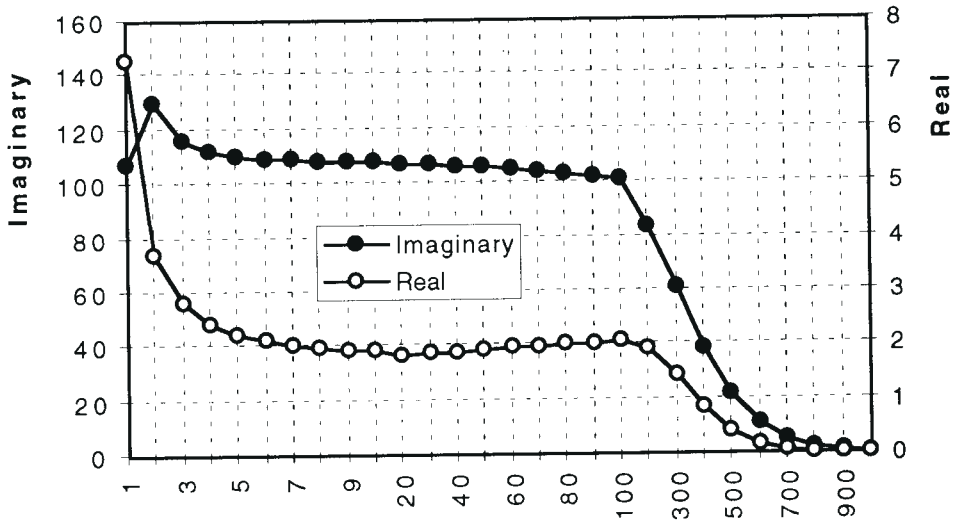


Figure 2. The longitudinal coupling impedance Z/n (in ohm) versus the harmonic number n

2.2 Transverse Coupling Impedance

There are four major contributions [13] to the transverse coupling impedance. Like in the longitudinal case, also here the space charge contribution dominates in a low-energy storage ring.

Space Charge:

$$Z_T = iR Z_0 \left( a^{-2} - b^{-2} \right) / \beta^2 \gamma^2 \qquad (10)$$

Wall Resistivity:

$$Z_T = (1 - i) R \left[ 2 R Z_0 \rho_w / \beta ( n - \nu ) \right]^{1/2} / b^3 \qquad (11)$$

Deflection Mode:

By virtue of the deflection theorem [13], the longitudinal coupling impedance estimate can be translated into an equivalent transverse coupling impedance

$$Z_T = 2 R Z / \beta b^2 ( n - \nu ) \qquad (12)$$

Finally there are transverse (as well longitudinal) parasitic modes due to several resonating structure, which are difficult to estimate, but that can be calculated with codes like MAFIA or measured with the beam itself.

Figure 3 gives the estimate of the transverse coupling impedance for the low-energy NSNS storage ring example. The large variation in correspondence of the low values of harmonic number is caused by the contribution of the resistive wall and of the deflection modes in proximity of the betatron tune.

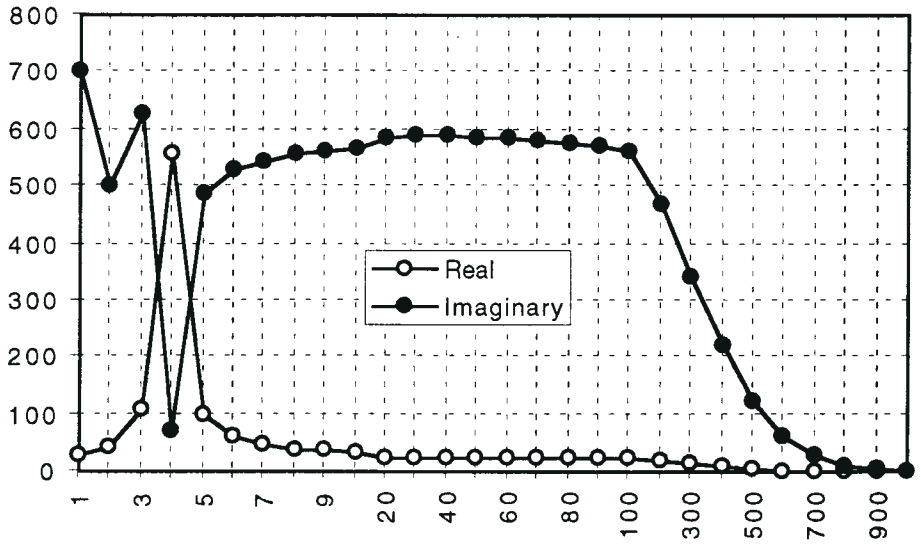


Figure 3. The transverse coupling impedance $Z_T$ (in kohm/m) versus the harmonic number n

## 3. Individual Bunch Instabilities

It is customary to divide these in the longitudinal, transverse and head-tail effects. We shall examine each of them below for the example of the NSNS storage ring described above. We like to point out that our case corresponds again to a low-energy storage ring operating well below the transition energy. Therefore results that are typical to high energy storage rings do not necessarily apply here.

### 3.1 Longitudinal Instabilities

There is a single long bunch. Coasting beam theory [6,14] is first applied by estimating the complex factor

$$U' - iV' = -i\, 2\, e\, I_p\, \beta^2\, (Z/n) / \pi\, |\eta|\, E\, (\Delta E/E)_{FWHM}^2 \qquad (13)$$

where $I_p$ is the bunch peak current and $\eta = \gamma_T^{-2} - \gamma^{-2}$

The so-called Keil-Schnell criterion seems to apply rather well for cases of accelerators and storage rings well above the transition energy when the dependence of the beam stability on the actual beam distribution function is not important. This is not the case well below the transition energy when it is more important to compare the actual dynamical value against the stability diagram for a give realistic distribution function.

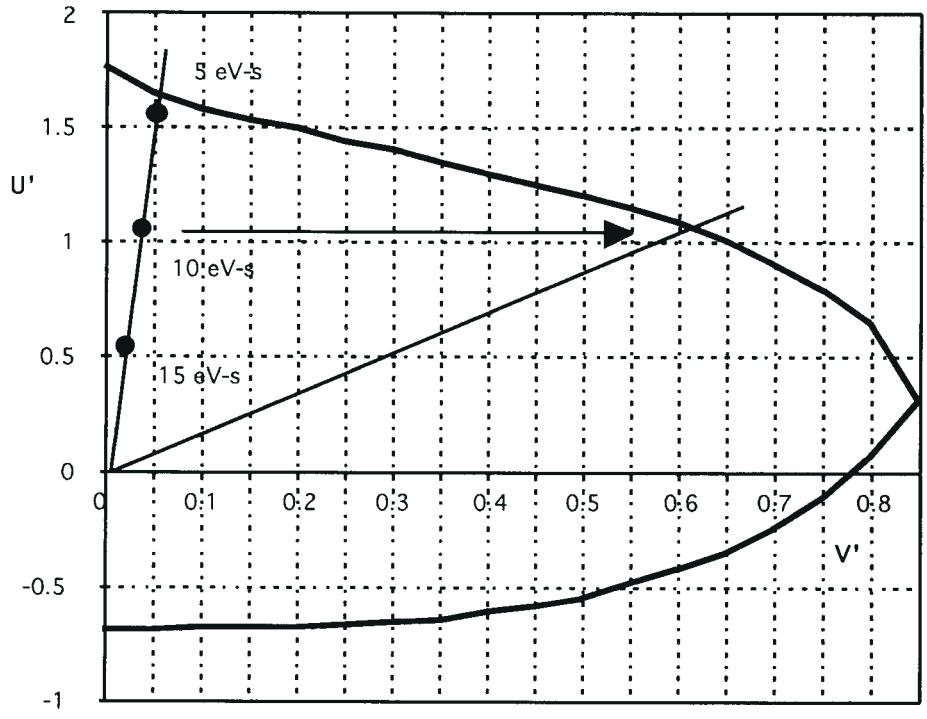


Figure 4. (U′, V′) stability diagram for cos-distribution

For our case, taking the space charge contribution and an inductive wall contribution of -i 20 ohm as well as a resistive contribution of 3 ohm gives U′= 1.1 and V′ = 0.02 which corresponds to a full momentum spread $\Delta p/p = 1.7$ %. Figure 4 shows the stability diagram in the (U′, V′) - space for a cos-distribution [14]. The working point is marked with a large black circle. It corresponds to a total bunch area of 10 eV-s. With this value the motion is stable. It is seen that there is plenty of safety margin for increasing, if required, the resistive contribution. Also, it is possible to include more wall components, as long they are of inductive nature so that they can subtract from the large space-charge contribution.

Even when the U′, V′ parameters fall outside the coasting beam stability area, there are two other conditions that are to be satisfied in order for the motion to be unstable. One is the so-called Hereward condition [15], that is the ratio of the instability growth rate to the synchrotron frequency should be less than unit. In our case this is 0.084 which clearly shows very little consequences from the synchrotron motion, and thus the beam continues to be stable. The other condition deals with the fact that the coasting beam theory was developed assuming only one mode at the time, that is that neighboring coherent modes are completely decoupled from each other. This is satisfied only if the real frequency shift is sufficiently small compared to the revolution frequency. Unfortunately the impedance imaginary part is very large, mostly because of the space-charge contribution due to the low energy of the beam. The real frequency shift is 3.5 times the revolution frequency so that several coherent modes are involved at the same time [16]. We do not have yet an understanding of this effect and whether there is a consequence to the beam stability.

### 3.2 Transverse Instability

Also in this case the method is the same. We first apply a coasting beam theory [17,18] stability condition given by

$$| Z_T | \; < \; E_0 \, \pi \, \nu \, \beta \, \gamma \, [ \, | \, (n - \nu)\eta + \xi \, | \, (\Delta p/p) \; + \; \delta\nu \, ] \; / \, e \, I_p \, R \; = \; Z_{beam} \qquad (14)$$

where $E_0$ is the proton rest energy, $\xi$ the accelerator chromaticity, and $\delta\nu$ the betatron tune spread from non linear elements like octupole magnets. We estimate also the growth rate of a potential instability in the limit of no Landau damping [13],

$$\tau^{-1} \; = \; I_p \, r_p \; \mathrm{Re} \, ( \, Z_T \, ) \, / \, e\nu \, \gamma \, Z_0 \qquad (15)$$

The growth time is plotted in Figure 5 versus the harmonic number. For $n < 100$, it is less than 0.2 ms which is considerably shorter than the synchrotron period of 1.2 ms, denoting thus the possibility of fast coasting beam-like instabilities.

The difference $|Z_T| - Z_{beam}$ is plotted in Figure 6 versus the harmonic number n. In absence of external betatron tune spread, $\delta\nu = 0$, the difference is negative for $n < 100$, denoting instability for these modes. For the motion to be stable at all modes one requires $\delta\nu = 0.11$. It is to be noted that the tune spread from the incoherent space-charge forces does not have a stabilizing effect on coherent oscillations.

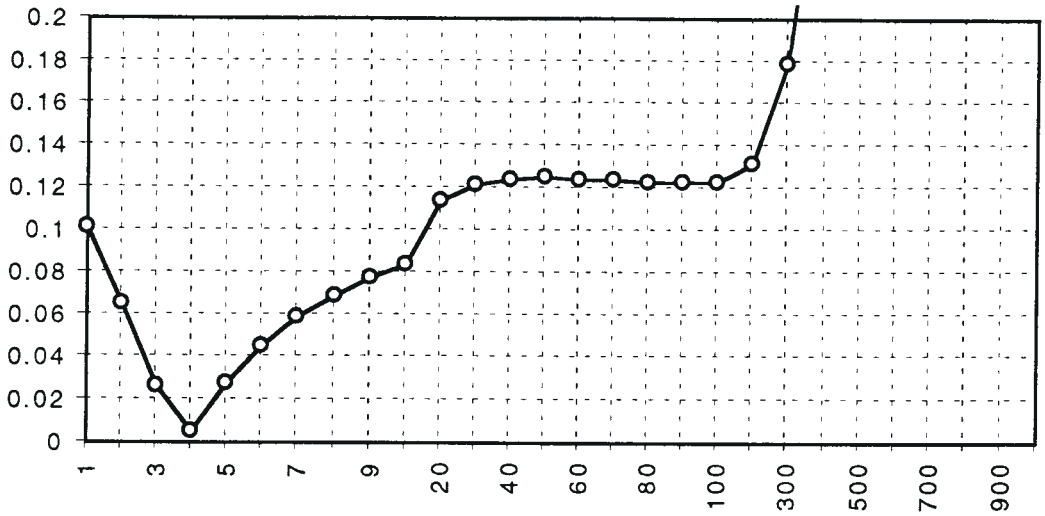


Figure 5. Growth time (ms) of transverse coherent instability in absence of Landau damping versus the harmonic number n

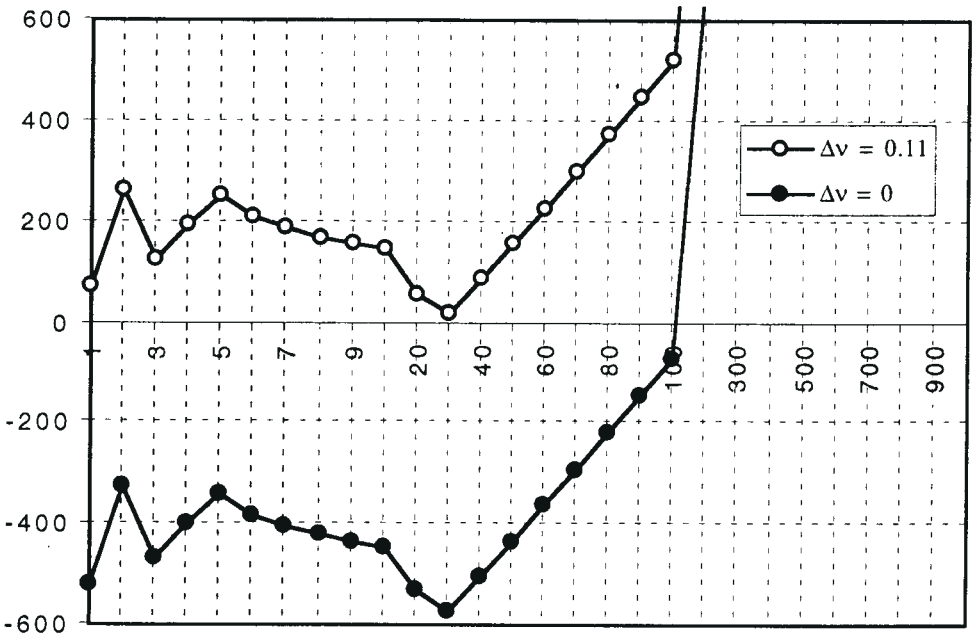


Figure 6. $|Z_T| - Z_{beam}$ in kohm/m versus the harmonic number n

### 3.3 Head-Tail Effect

The only other concern left is the possibility of slow head-tail instabilities [19], for which the stability criterion (14) does not apply. This type of instability is caused by the transverse betatron motion coupled to the synchrotron motion. It may occur only when the growth rate is comparable

or lower than the synchrotron frequency. The parameter of relevance is the accumulated betatron phase shift

$$\chi = 2\pi\xi \nu f_0 \tau_L / \eta \tag{16}$$

where $\tau_L$ is the bunch length in time units. For the case of uncorrected chromaticity this quantity is positive and large (we are constantly below transition energy and $\xi < 0$), ranging around 60. The head-tail mode numbers m which are stable, also in the absence of Landau damping, can be estimated from the condition $m < \chi / 2\pi$, which gives $m < 10$. Thus the head-tail instability is unlikely to appear in the accumulator ring. Moreover, as we have seen, a significant large tune spread will be provided with octupole magnets to stabilize the beam against fast transverse coherent oscillations, and this spread will stabilize the beam also against slow transverse oscillations caused by a head-tail type of instability.

## 4. Incoherent Space-Charge Effects

The space charge effects are particular important in NSNS, owing to the relatively low injection energy, and also the allowed low level of the beam loss. The maximum incoherent tune spread is estimated by,

$$\Delta\nu = N r_p / 2 B_f \beta^2 \gamma^3 \varepsilon \tag{17}$$

where N is the total number of particles, $r_p = 1.535 \times 10^{-18}$ m, and $\varepsilon$ is the full un-normalized beam emittance which can be taken as 5 times the rms emittance. The bunching factor $B_f$ is defined as the ratio of the average beam current over the peak current. To avoid arbitrary cuts and discontinuity of the distribution at the tail, we have adopted a square-cosine type of distribution with $\tau_L$ the total bunch length. The bunching factor for such a distribution can be easily estimated,

$$B_f = 0.5 \tau_L f_0 = 0.32 \tag{18}$$

We note that in the NSNS there is only one single bunch. The resulting tune spread for the NSNS is 0.2. In practice this value is expected to be lowered by the flattening effect of the longitudinal space charge forces. Moreover, a tune spread of about half the space charge depression is needed to be created with octupoles to stabilize the beam against transverse coherent oscillations. The octupole polarity can be chosen in such a way the corresponding tune spread actually subtract from the space charge value yielding an overall spread of about 0.1.

Other approaches can be considered to reduce further the tune spread. One is the use of a second harmonic rf system to flatten the distribution toward larger values of the bunching factor. The second method is to adopt the "painting" technique during injection to shape the beam toward a more rectangular transverse distribution. There are nevertheless concerns about the attainment of these flattened distributions since they can cause disruptive effects of coherent instability both in the longitudinal and transverse plane.

## 5. References


[1] J. Alonso, The NSNS Project, contribution to EPAC 96, Barcellona, Spain. June 1996.
[2] The impedance estimate has been done with ZOVERN, a program written by A.G. Ruggiero,
[3] A. Sessler and V.G. Vaccaro, Internal Yellow Report, CERN 67-2, Feb. 1967.
[4] C.E. Nielsen et al., Proc. of Int. Conf. on High Energy Accel., 239, CERN 1959.
[5] A. Faltens and L.J. Laslett, Proc. of the 1975 ISABELLE Summer Study, vol. II, p. 486.
[6] V.K. Neil and A.M. Sessler, Rev. Sci. Instr., 36, 429 (1965).
[7] R. Briggs and V. Neil, Plasma Physics 8, 255 (1966).
[8] A.G. Ruggiero, Fermilab Technical Notes FN-219, FN-220 and FN-230. (1970-71).
[9] E. Keil and B. Zotter, Particle Accelerators, vol. 3, pp. 11-20. (1972).
[10] A.G. Ruggiero, V.G. Vaccaro and P. Strolin, CERN ISR-RF-TH / 69-7. (1969).
[11] H.G. Hereward, CERN / ISR - DI / 75-47. (Oct. 1975).
[12] M. Sands, SLAC/PEP Internal Report, 1980 (?)
[13] F. Sacherer, Proc. of 9th Int. Conf. on High Energy Accel., SLAC, 347, (May 1974).
[14] A.G. Ruggiero and V.G. Vaccaro, CERN - ISR - TH / 68-3, July 1968.
[15] H.G. Hereward, Proc. of the 1975 ISABELLE Summer Study, vol. II, p. 555.
[16] F. Sacherer, IEEE Trans. on Nucl. Sci., vol. NS-24, no. 3, 1393 (June 1977).
[17] L.J. Laslett, V.K. Neil, A.M. Sessler, Rev. Sci. Instr., 36, 436, (1965).
[18] K. Hubner, A.G. Ruggiero, V.G. Vaccaro, Proc. 7th Int. Conf. on High Energy Accel., Yerevan, p. 343 (1969).
[19] C. Pellegrini, Nuovo Cimento, 64A, 477 (1969).